Journal of Theoretical and Applied Information Technology
15th November 2012. Vol. 45 No.1

ISSN: 1992-8645 www.jatit.org E-ISSN: 1817-3195

ENSEMBLE MODELING OF MILL LOAD BASED ON EMPIRICAL MODE DECOMPOSITION AND PARTIAL LEAST SQUARES

[1,2]LIJIE ZHAO, [2, 3]JIAN TANG, [4]WENGRONG ZHENG

[1] College of Information Engineering, Shenyang University of Chemical Technology, Shenyang 110042, Liaoning, China

2 State Key Laboratory of Synthetical Automation for Process Industries, Northeastern University, Shenyang 110819, Liaoning, China

[3] Unit 92941, PLA, Huludao, China

[4] Naval University of Engineering, Wuhan 430032, Hubei, China

ABSTRACT

Reliable measurements of ball mill load parameters and reorganization of the operating statuses are the key factors for saving energy and optimization control. Empirical mode decomposition (EMD) and partial least squares (PLS) are used to analyze shell vibration signal and monitor mill load parameters of ball mill. The shell vibration signal is decomposed into several intrinsic mode functions (IMFs) adaptively. The power spectral density (PSD) of each IMF is analyzed under different grinding conditions. A new index is defined to measure the relative change of each IMF to original signal, which is also used to select more informational IMFs. The ensemble PLS method is used to build soft-sensor models based on frequency spectrum of the selected IMFs. Experimental results show that ensemble soft-sensor model based on EMD and PLS can extract effective features of shell vibration signal and monitor mill load effectively.

Keywords: *Parameters Estimation, Vibration Signal Analysis, Empirical Mode Decomposition; Partial Least Squares, Ensemble Modeling*

1. INTRODUCTION

Ball mill load is the most important information in the mineral processing, which is also one of the key factors for the implement of the optimization and control of the grinding process. The parameters and condition of the ball mill load are closely related to grinding process operating efficiency, product quality and energy consumption. However, communication mechanism of wet ball mill is still far from understood [1]. It is difficult to online measure the mill load for poor conditions inside ball mills because of a series of complex impact and grinding among steel balls and materials, steel balls and lining [2].

Mill load parameters inside ball mill including material to ball volume ratio (MBVR), pulp density (PD) and charge volume ratio (CVR) have direct relationship with the grinding production ratio [3]. Zeng et al. constructed the partial least square (PLS) and principle component regression (PCR) models between PD and characteristic frequency sub-bands based on the spectrum of axis vibration and acoustical signals of the ball mill [4]. However, the axis vibration signal is dispersed and disturbed by the transfer system of ball mill, and the acoustic signal has acoustical crosstalk with adjacent mill. Shell vibration signal is more sensitive than the acoustical signal and has fewer disturbances [5]. The studies of the shell vibration for a semi-autogenous (SAG) mill show that shell vibration is indicator of pulp density and viscosity [6]. Recently, tang et al. make a detail experimental research on a laboratory scale ball mill [7], which shows that the mill load parameters have stronge relationship with the shell vibration frequency spectrum. A genetic algorithm-partial least square (GA-PLS) based modeling method has been proposed. However, it is difficult to explain the physical meaning of the selected sub-bands and is time-consuming due to the random initialization of GA. A principal component analysis-support vector machines (PCA-SVM) approach was proposed in [8] to modeling these mill load parameters. However, principal components don't take into account the correlation between inputs and outputs [9]. Combined with the mechanical analysis of the shell vibration production, PLS and adaptive weighting fusion algorithm [10] based on ensemble modeling method is proposed. However, the

ISSN: 1992-8645 www.jatit.org E-ISSN: 1817-3195

partition of the frequency bands is manual, and some sub-models have higher predication accuracy than the ensemble model.

In fact, the mill shell is impacted by a variety of impact forces with different amplitudes and frequencies. It is essential to split the shell vibration signal into different sub-signals which maybe caused by different vibration resources and contain different information on mill operation. Empirical mode decomposition (EMD) was proposed by Huang [11], which is a self-adaptive method based on partial characteristic of the signal. It essentially allows the decomposition of the time-domain original signals into some intrinsic mode functions (IMFs), and provides a time-frequency distribution. This method has been widely used in fault diagnosis [12]. By analyzing each IMF component that involves the local characteristic of the signal, the characteristic information of the original signal could be extracted more accurately and effectively. Thus, the EMD and power spectral density (PSD) methods were used to analyze the shell vibration signal by using PCA and PLS algorithm respectively [13]. However, it was weak on analysis of shell vibration and prediction performance of models for mill load parameters. How to analyze the IMFs and how to improve the modeling accuracy is still an open issue.

Therefore, EMD and ensemble PLS based modeling technology is proposed. At first, the original shell vibration signal is decomposed into a number of intrinsic mode functions (IMFs) adaptively using EMD technology. Then, the power spectral density (PSD) of each IMF is analyzed in detail under different grinding conditions and a new index is defined to select more informational IMFs. Finally, the ensemble PLS method is used to construct soft-sensor models based on frequency spectrum. Experiments are done on a laboratory ball mill to validate this approach.

This paper is organized as follows: Section 2 presents the materials and method using in this paper, section 3 focuses on the experiment results and discussion, section 4 gives the conclusions

2. MATERIALS AND METHOD

2.1 Experimental Descriptions

The experiments were performed on a laboratory scale ball mill (XMQL-420×450) which is a continuous grinding grid ball mill. The mill, driven by a three-phase 2.12kW motor, has a maximum ball load of 80kg, a designed pulverizing capacity of 10kg per hour, a rated speed of 57 revolution per minute and volume of 60 L of drums . The copper ore, which is used as material to be pulverized, is crushed to about less than 6 mm before used. The diameters of the steel balls are 30 mm, 20 mm and 15 mm with the ball radius ratio of 3:4:3, respectively. The shell vibration signals of the mill operated under four grinding conditions, as illustrated in Table 1, as shown in [7].

Table 1: Experimental Detail Of Four Grinding Conditions

	Grinding conditions	running time (s)	Times (n)	Mill load (kg)						Increase steps (kg)
				ball				mineral	water	
				Big	Medium	Small	All balls			
1	Ball	60	15	0	0	10~80	10~80	0	0	5
		60	3	0	20~80	0	20~80	0	0	30
		60	2	22~50	0	0	22~50	0	0	28
2	Ball-Mineral	120	5	20	10	10	40	10~40	0	10
		120	3	6~18	8~24	6~18	20~60	10	0	6,8,6
3	ball-Water	30	6	6	8	6	20	0	5~50	5,10
4	Ball-Mineral-Water	60	6	12	16	12	40	10	5~40	5,10
		60	7	12	16	12	40	20	2~20	3,2,5
		60	9	12	16	12	40	22~50	10	2,5
		60	6	12	16	12	40	10~20	2	2
		60	6	6~9	8~16	6~12	20~37	4	5	3,4,3

2.2 Methods

The mechanical grinding process of ball mill produces strong vibration and acoustic signals, which are stable and periodic over a given time interval. The vibration acceleration signals of the mill shell are sensitive to the impact force of mill load to mill liners. If we analyze the shell vibration signal in one rotation of ball mill, the original shell

Journal of Theoretical and Applied Information Technology
15th November 2012. Vol. 45 No.1

ISSN: 1992-8645 www.jatit.org E-ISSN: 1817-3195

vibration signals can be decomposed to different sub-signals. Every sub-signal is an IMF of the EMD decomposition. Every IMF maybe caused by different reasons and contains different information. Studies show that the relative amplitudes of the vibration frequency spectrum contain information directly relate to the operating parameters of grinding process. Then, the frequency spectrum of the IMF can embody the information more evidently. Comparing to the spectrum of the IMFs and the original signals, we can understand the grinding mechanism and the composition of the shell vibration signal more deeply.

A method combining EMD, FFT, PLS and ensemble modeling technologies is proposed to analyze the shell vibration signal and monitor the parameters of mill load, as shown in Fig.1.

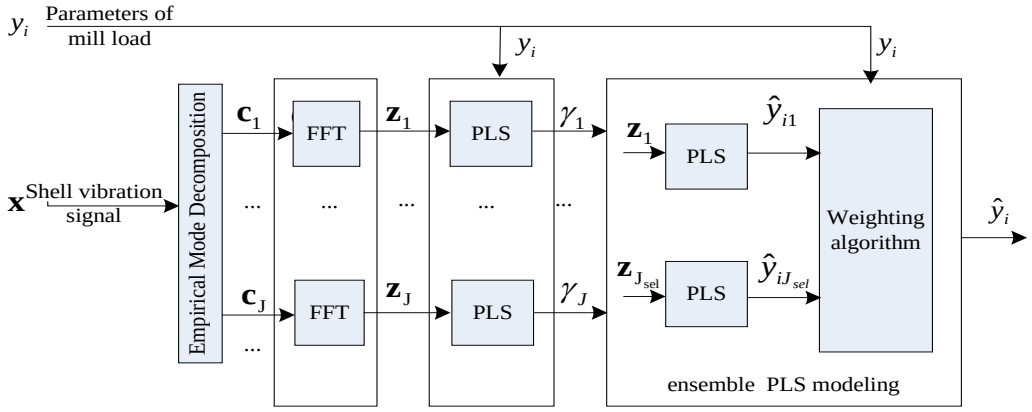

Figure 1: EMD And PLS Based Modeling Approach

In Fig.1, $\mathbf{x}$ represents the original shell vibration signal; $\mathbf{c}_j$ represents the jth IMF, where $j = 1, \cdots, J$, J is the number of the IMFs; $\mathbf{z}_j$ represents the frequency spectrum of the jth IMF; γ_j is the relative change coefficients of the jth IMFs to the original signal; $\mathbf{z}_{j_{sel}}$ represents the frequency spectrum of the j_{sel}th IMF for construct ensemble PLS model, where $j_{sel} = 1, \cdots, J_{sel}$, J_{sel} is the number selected IMFs; y_i represents the parameters of mill load, where $i = 1, 2, 3$ represents mineral to ball volume ration, pulp density and charge volume ratio respectively.

2.2.1. Empirical mode decomposition based signal adaptive decomposition

The EMD technology can directly analyze the original signal according to the interior time scale of data. Therefore, EMD can decompose a non-linear and non-stationary data into a sequence of amplitude-modulation/frequency-modulation components. However, it is based upon three assumptions [14]: (1) The signal has at least two extreme (maximum and minimum); (2) The characteristic time scale is defined by the time lapse between successive alternations of local maxima and minima of the signal; (3) If the signal has no extreme but contains inflection points, then it can be differentiated once or more times to reveal the extreme.

The amplitude-modulation / frequency-modulation components are called as IMFs that must satisfy the following two conditions [15]: (1) In the whole data set, the number of extreme and the number of zero-crossings must either be equal or differ at most by one; and (2) At any point, the mean of the envelope defined by local maxima and the envelope defined by local minima are zero.

The procedure of EMD method is a sifting process iteratively. The decomposition of shell vibration signal is as follows:

Step1: Assume that $x(t)$ is the original signal. Find out the entire extreme of the signal.

Step2: Connect all the local maxima and minimum by a cubic spline as the upper and lower envelope respectively. The upper and lower envelopes should cover all the data between them.

Step3: Calculate the mean value of the upper and low envelope value. It is designated as m_1, the difference between the original signal $x(t)$ and m_1 are the first component h_1.

ISSN: 1992-8645 www.jatit.org E-ISSN: 1817-3195

$$h_1 = x(t) - m_1 \quad (1)$$

Step4: Check whether h_1 satisfy the IMF criteria or not. Ideally, if h_1 is an IMF, then h_1 is the first component of $x(t)$.

Step5: If not, the above procedure Step1)-Step 3) repeat. Here h_1 is treated as the original signal, then

$$h_{11} = h_1 - m_{11} \quad (2)$$

where m_{11} is the mean of upper and low envelope value of h_1. This process can be repeated up to k times, until h_{1k} becomes an IMF, that is

$$h_{1k} = h_{1(k-1)} - m_{1k}. \quad (3)$$

After each sifting processing, it is necessary to check whether the number of zero crossings equals to the number of extreme. The finally of component is made as the first IMF, and then it is designated as

$$c_1 = h_{1k}. \quad (4)$$

where c_1 should contain the finest scale or the shortest period component of the signal.

Step6: Next, separate c_1 from the original $x(t)$, which could get:

$$r_1 = x(t) - c_1. \quad (5)$$

Here r_1 is treated as the original data, and by repeating the above processes, the second IMF component c_2 of $x(t)$ could be obtained. Thus repeat the process above j times, then jth-IMFs of signal $x(t)$ could be obtained.

As soon as r_j becomes a monotonic function, the decomposition process can be stopped and there is no more IMFs can be extracted from the signal. Following the process above, the equation below is gained:

$$x(t) = \sum_{j=1}^{n} c_j + r_n. \quad (6)$$

Thus, the signal $x(t)$ is decomposed into n-IMFs, which include different frequency bands ranging from high to low and a residue r_n which can be either the mean trend or a constant.

2.2.2 Time/frequency transform

Although the IMFs of the shell vibration are obtained, the interested signals for the grinding status cannot be extracted evidently. The frequency spectrum has direct relationship with the operating parameters inside ball mill. After decomposition the original data into several IMFs, the classic Welch's method is used to obtain the PSD of each IMF respectively. The data length to obtained PSD should be one revolution of the ball mill. Moreover, the finial PSD should be averaged by several revolutions to overcome the fluctuation of the operating conditions.

Denote the frequency spectrum of c_j as $\mathbf{z}_j$, where j indicates the jth-IMF. The relationship between $\mathbf{z}_j$ and mill load parameters would be analyzed in detail for interpretation the vibration signal more deeply.

2.2.3 Partial Least Squares based frequency spectrum analysis

Partial least squares (PLS) is a multivariate projection method, which can capture the maximal covariance between the input variables and output variables using the latent variables by decomposing the input and output variables simultaneously [16]. Assume predictor variables $Z \in \Re^{n\times p}$ and response variables $Y \in \Re^{n\times q}$ are normalized as $E_0 = \left(E_{01} \quad E_{02} \quad \cdots \quad E_{0p}\right)_{n\times p}$ and $F_0 = \left(F_{01} \quad F_{02} \quad \cdots \quad F_{0q}\right)_{n\times q}$ respectively. Let t_1 be the first latent score vector of E_0, $t_1 = E_0 w_1$, and w_1 be the first axis of the E_0, $\| w_1 \| = 1$. Let u_1 be the first latent score vector of F_0, $u_1 = F_0 c_1$, and $\mathbf{c}_1$ be the first axis of the F_0, $\| c_1 \| = 1$.

We want to maximize the covariance between $t_1 = E_0 w_1$ and $u_1 = F_0 c_1$, thus have the following optimization problem:

$$\begin{aligned} &Max < E_0 w_1, F_0 c_1 > \\ &s.t. \quad w_1^T w_1 = 1, c_1^T c_1 = 1 \end{aligned} \quad (7)$$

By solving (7) with the Lagrange approach,

$$s = w_1^T E_0^T F_0 c_1 - l_1(w_1^T w_1 - 1) - l_2(c_1^T c_1 - 1) \quad (8)$$

where λ_1 and $\lambda_2 \geq 0$. At last, we obtain that $\mathbf{w}_1$ and $\mathbf{c}_1$ are the maximum eigenvector of matrix $E_0^T F_0 F_0^T E_0$ and $F_0^T E_0 E_0^T F_0$. So, after t_1 and u_1 is obtained. We have $E_0 = t_1 p_1^T + E_1$, $F_0 = u_1 q_1^T + F_1^0$ and $F_0 = t_1 b_1^T + F_1$. In which, $p_1 = \frac{E_0^T t_1}{\| t_1 \|^2}$, $q_1 = \frac{F_0^T u_1}{\| u_1 \|^2}$, $b_1 = \frac{F_0^T t_1}{\| t_1 \|^2}$, and E_1, F_1^0

ISSN: 1992-8645 www.jatit.org E-ISSN: 1817-3195

and F_1 are the residual matrices. Then we replace E_0 and F_0 with E_1 and F_1 to obtain the second latent score vectors t_2 and u_2. Using the same method, we get all the latent score vectors until $E_h = F_h = 0$.

Therefore, the PLS decomposes the data matrices Z and Y into a low dimensional space with h latent variables, which can be show as follows:

$$Z = TP^T + E \quad (9)$$

$$Y = UQ^T + F \quad (10)$$

where $T = [t_1, t_2, ..., t_h]$ and $U = [u_1, u_2, ..., u_h]$ are score matrice; $P = [p_1, p_2, ..., p_h]$ and $Q = [q_1, q_2, ..., q_h]$ are loading matrices respectively. E and F are the modeling residual of Z and Y. These two equations can be written as a multiple regression model:

$$Y = ZB + G \quad (11)$$

where matrix B contains the PLS regression coefficients and can be calculated as follows:

$$B = Z^T U(T^T ZZ^T U)^{-1} T^T Y \quad (12)$$

In order to show the relative change coefficients of the IMFs to the original signal, a new index is defined as following:

$$\gamma_{\mathrm{IMF}} = \frac{c_{\mathrm{jIMF}}}{c_{orig}} \quad (13)$$

where c_{jIMF} and c_{orig} represents the frequency spectral correlate coefficients of the jth IMF and original signal. If the value of γ_{jIMF} is larger than one, which shows it contains more information than the original signals. Then we can select IMFs with higher γ_{jIMF} to construct models for monitoring mill load parameters.

2.2.4 Ensemble PLS based mill load parameters modeling

It is possible to monitor mill load parameters according to the selected IMFs. Due to robust to high dimensional, collinear, and noise in data set, PLS is used to build soft sensor models of mill load parameters. Ensemble methods have received special attentions because it can improve accuracy of the predictor and achieve better stability through building a set of individual models, with the goal of reducing the expected error of the model [17]. To build an ensemble, a set of diverse ensemble components and combination mechanism of their predictions are needed to obtain the final ensemble model. Ensemble PLS (EPLS) approach is proposed to model near-infrared complex spectral data [18]. This approach involves three steps: (1) Training a pool of PLS sub-models individually; (2) Selecting some PLS sub-models; and (3) combining the selected PLS sub-models to get the final predictions of mill load parameters.

We construct sub-models of mill load parameters with frequency spectrum of different IMFs, and then use adaptive weight fusion to weight these sub-models. The estimate value of ensemble PLS models can be calculated by:

$$\hat{y}_i = \sum_{j=1}^{J_{\mathrm{sel}}} w_{ij} \hat{y}_{ij} \quad (14)$$

where $i = 1, 2, 3$ represent material to ball volume ratio, pulp density and charge volume ratio respectively; J_{sel} is the numbers of the selected sub-models; $\hat{y}_i$ and $\hat{y}_{ij}$ are the estimate value of the ensemble PLS model and the jth sub-model for the ith mill load parameter ; $\sum_{j=1}^{J_{\mathrm{sel}}} w_{ij} = 1, 0 \le w_{ij} \le 1$, w_{ij} is the weight coefficients of the jth sub-model for the ith mill load parameter. It is calculated based on [15]:

$$w_{ij} = 1 \Big/ \left((\sigma_{ij})^2 \sum_{j=1}^{J_{sel}} \frac{1}{(\sigma_{ij})^2} \right) \quad (15)$$

where σ_{ij} is the standard variance of the estimate value $\{\hat{y}_{ij}^l\}(l = 1, 2, \cdots, n)$.

3. RESULTS AND DISCUSSION

3.1 Empirical Mode Decomposition Of Shell Vibration Signal

3.1.1 Intrinsic mode functions under extreme grinding conditions

Power spectrum of each IMF of shell vibration signals is calculated by using classics Welch power spectrum estimation methods. The time/frequency domain curves of the IMFs under different grinding conditions are shown in Fig.2.

Journal of Theoretical and Applied Information Technology
15th November 2012. Vol. 45 No.1

ISSN: 1992-8645 www.jatit.org E-ISSN: 1817-3195

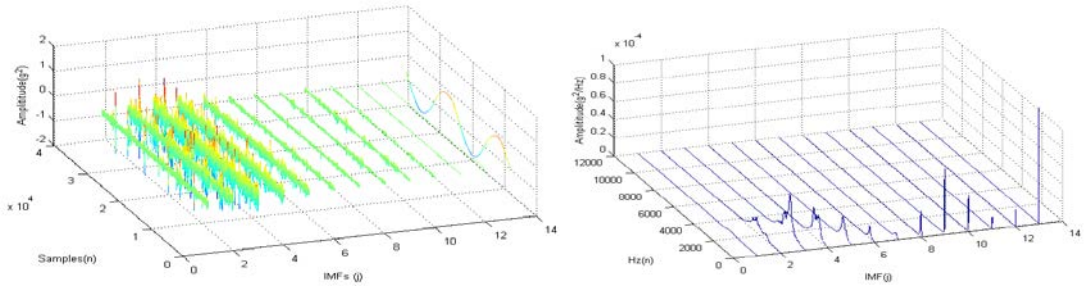

(A) Time/Frequency Domain Curves Of The Imfs Under Zero Load Condition

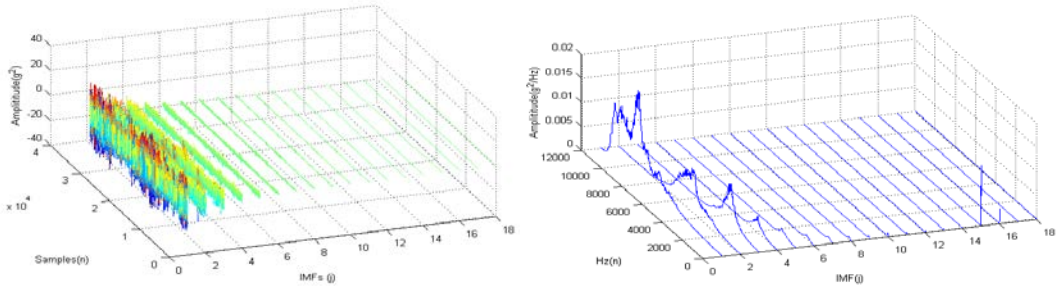

(B) Time/Frequency Domain Curves Of The Imfs Under Ball Load Condition

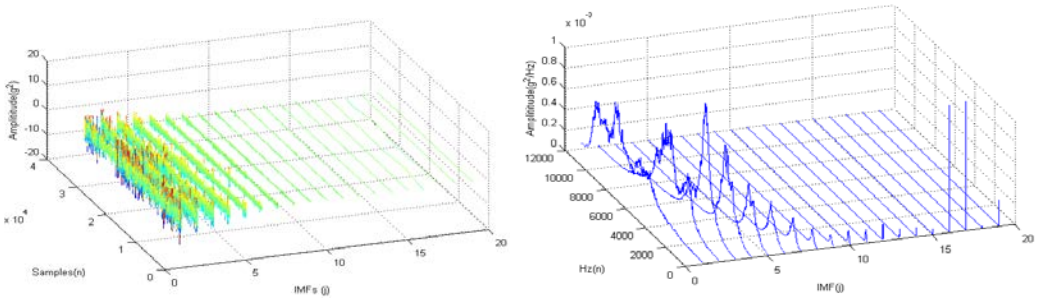

(C) Time/Frequency Domain Curves Of The Imfs Under Ball And Water Load (Water Grinding) Condition

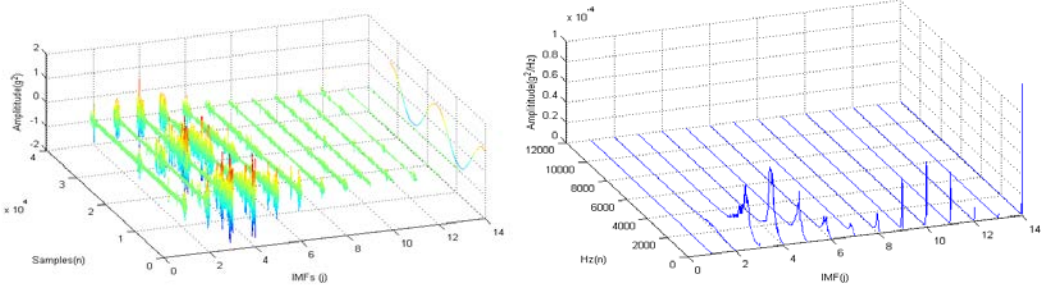

(D) Time/Frequency Domain Curves Of The Imfs Under Ball And Mineral Load (Dry Grinding) Condition

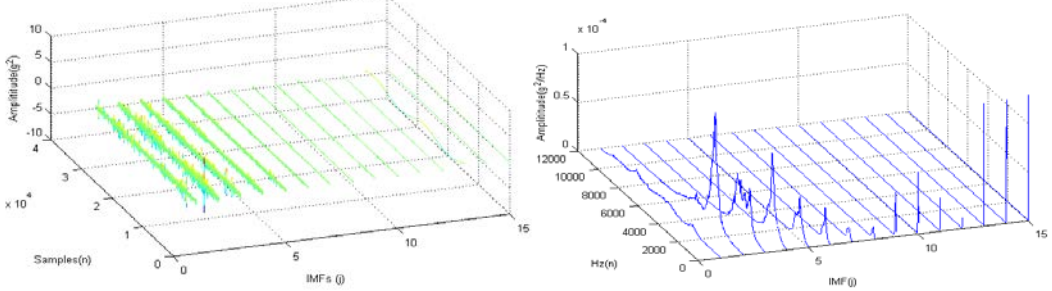

(E) Time/Frequency Domain Curves Of The Imfs Under Ball, Mineral And Water Load (Wet Grinding) Condition

Figure 2 Time/Frequency Domain Curves Of The Imfs Under Different Grinding Conditions

ISSN: 1992-8645 www.jatit.org E-ISSN: 1817-3195

The load in Fig .2 are: ball load 40kg, mineral load 30kg and water load 10kg. The experiments are performed with the different grinding conditions such as: (a) zero load; (b) ball load; (c) ball and water load; (d) ball and mineral load; (e) ball, water and mineral load. Fig .2 shows the shell vibration signals under different grinding conditions can be decomposed to lots of IMFs with different time-domain and frequency-domain features. The following results are shown:

(1) The rotation of the ball mill is one of the sources of the mill shell vibration for this laboratory-scale ball mill. On zero load grinding condition, the 13th IMF is a periodical signal with the highest amplitude, whose frequency is the rotating frequency of the ball mill shell. Thus, the 13th IMF is caused by the rotating of the mill shell. This shows that there is a mass equivalent with this experimental ball mill itself. Moreover, the frequency spectrum of the 13th IMF is 122 times the 3rd IMF's.

Remark: In order to display the other IMFs' spectrum, the up limit of the "z axis" in Figure 2(a) is limited at 0.0001. The similar operations are done in other figures except Figure 2(b). Thus, we cannot plot the 13th IMF totally. On the only ball load condition as shown in Figure 2(b), the shell vibration is so strong that the rotation periodical signal cannot be seen clearly. .

(2) The different characters of the water, the mineral and the pulp affect the impaction of balls to liners by various energy dissipation mechanisms, which decide the different shapes of the IMFs in time domain and frequency domain. The maximum amplitudes of the time-domain IMFs are 2, 40, 20, 2 and 10 for (a), (b), (c), (d) and (e) of Figure 2 respectively. With only ball load condition, no any damping medium exists; the balls impact the mill shell directly and strongly. Thus, the biggest amplitude is obtained, and the vibration frequency is mainly medium and high frequency bands. With the adding of the water in Figure 2(c), water and mineral in Fig .1 (e), and the mineral in Fig 1.(d), the mainly vibration source become the rotation of the mill shell. That is to say, the impactions of the balls to the mill liners are damped. The difference of grinding mechanism for dry milling and wet milling can also be shown in the frequency spectrum of these IMFs.

(3) Different IMfs contain different information. It is possible to select some useful IMFs to construct more effective soft sensor models. However, the details explanation of the IMFs should be done by integrating the finite element analysis of ball mill shell vibration system and more experiments.

3.1.2 Intrinsic mode functions under the wet grinding conditions

In practice, the motion of the steel ball is a three-phase hybrid movement, whose trajectory includes circular path, parabolic path and attracting path. Therefore, the mill shell is impacted by a variety of impact forces. In the wet ball mill of the grinding process, the motion of the balls is affected by the mill load parameters. For example, material to ball volume ratio, pulp density and viscosity affect the buoyancy and viscous effect to balls, and the coating thickness of the balls, and charge volume ratio affects the motion time of the balls in the pulp. Discrete element analysis based on the single steel ball shows that the friction coefficient between the steel ball and mill liner decides the "shoulder" zone of the ball leaving the mill liner and the "toe" zone of the ball dropping; the rebound coefficient between the balls and mill liner decides the rebound velocity [19]. Actually, both the two coefficient are affected by the mill load parameters. There are a large number of balls in the mill. These balls are layered, and balls in different layers are thrown down at the same time with different impact forces. The radius of the balls are different, thus the impact forces are also different. The hardness, particle distribution of the ore also affects the impact force. Under different pulp viscosity, the buoyancy and viscous effect to the balls are different. On some grinding conditions, the impact forces are difficult to a description. Thus, these impact forces with different sources and frequencies overlay each other . Therefore, the shell vibration signal can reflect the mill load parameters more accurately.

Based on the above analysis, we give the power spectral density (PSD) of different IMFs under different grinding conditions. The waterfall of the first six IMFs with only water, mineral and ball load change are analyzed and discussed in here.

3.1.2.1 Water-only load change

The mill was operated with the ball load at 40kg and mineral load at 10kg, but the water load was increased from 5kg to 40kg, the pulp density was decreased from 66.7% to 20%, and the charge volume ratio was increased from 20.1% to 79.1%. The PSD waterfalls the first six IMFs are shown in Figure 3.

Journal of Theoretical and Applied Information Technology
15th November 2012. Vol. 45 No.1

ISSN: 1992-8645 www.jatit.org E-ISSN: 1817-3195

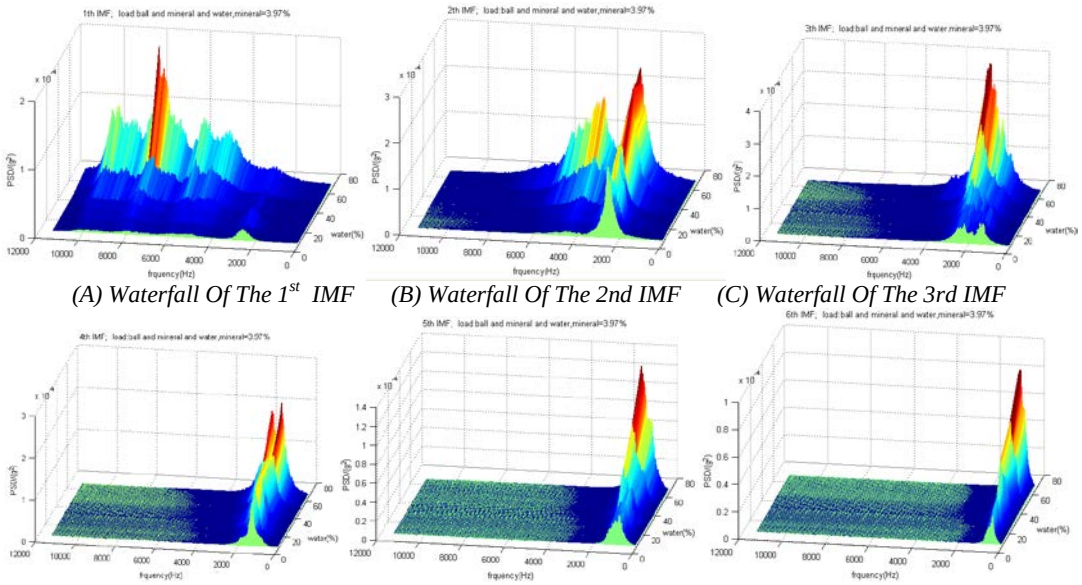

(A) Waterfall Of The 1st IMF (B) Waterfall Of The 2nd IMF (C) Waterfall Of The 3rd IMF

(D) Waterfall Of The 4th IMF; (E) Waterfall Of The 5th IMF; F) Waterfall Of The 6th IMF

Figure 3: PSD Waterfalls Of The Former Six Imfs With Water Load Increase

Initially, water is so little that pulp density is high. The amplitudes of the former six IMFs increase gradually with the increase of the water load. Initially, there is so little water and the pulp density is the largest. Then, with the increase of the water, pulp density and viscosity decreases, and the coating thickness of the balls also decreases, so the cushion function of the pulp decreases, thus enforces the impact between balls to mill shell. This is same as the previous conclusion [11]. The band width of the 1st IMF is mainly 4,000~12,000Hz, which maybe caused by the impact among balls. The band width of the 2nd and 3rd IMFs is mainly 2,000~6,000Hz, which may be caused by the impact of balls to liners. The 4th, 5th and 6th may correlate with the natural vibration frequency of the shell vibration system. These conclusions are only based on the quality judgment. However, all these results show that the original vibration signals can be decomposed to different parts, and each part is changed with the increase of the water load. It is useful to select some IMFs to construct more effective models.

3.1.2.2 Mineral-only load change

The mill was operated with the ball load at 40kg and water load at 10kg, but the mineral load was increased from 22kg to 50kg, and pulp density was increased from 68.8% to 83.3%, and charge volume ratio was increased from 34.6% to 45.0%. The PSD waterfalls of the former six IMFs are shown in Figure 4.

Journal of Theoretical and Applied Information Technology
15th November 2012. Vol. 45 No.1

ISSN: 1992-8645 www.jatit.org E-ISSN: 1817-3195

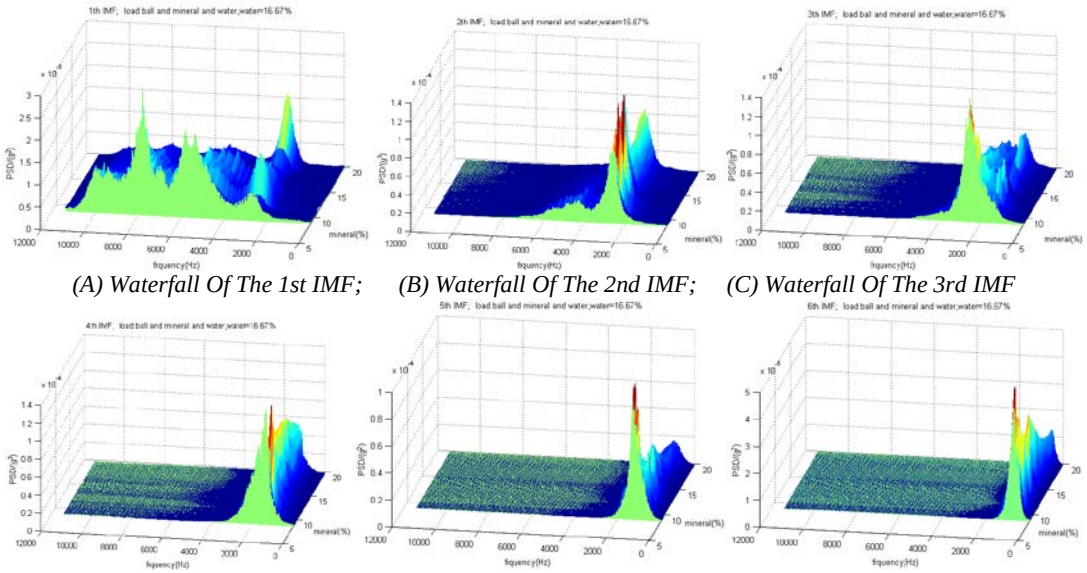

(A) Waterfall Of The 1st IMF; (B) Waterfall Of The 2nd IMF; (C) Waterfall Of The 3rd IMF

(D) Waterfall Of The 4th IMF; (E) Waterfall Of The 5th IMF; (F) Waterfall Of The 6th IMF

Figure 4: PSD Waterfalls Of The Former Six Imfs With Mineral Load Increase

Fig.4 shows that the ranges of the band width of different are same as Fig.3. Fig.4 (d), Fig.4 (e), and Fig.4 (f) show that with the increase of the mineral load, the amplitudes decrease rapidly with mineral load increasing from 22kg to 30kg, but slowly from 30kg to 50kg. Note that when the mineral load is 30kg, the corresponding pulp density is 75%. This is because the coating thickness of the balls does not increase evidently with the increase of pulp density when the density is higher than 75%, which makes the cushion functionality between balls to mill liners and balls to balls do not improve any more, and the impact to mill shell does not change. This is same as the previous conclusion [11]. However, Fig.4 (a), Fig.4 (b) and Fig.4 (c) don't embody this fact. Thus, more experiments and simulations should be done to solve this problem.

3.1.2.3 Ball-only load change

The mill was operated with the mineral load at 4kg and water load at 5kg, but the ball load was increased from 20kg to 37kg, and charge volume ratio was increased from 14.2% to 18.6%, and the medium charge ratio was increased from 10.1% to 18.6%. The PSD waterfalls of the former six IMFs are shown in Figure 5.

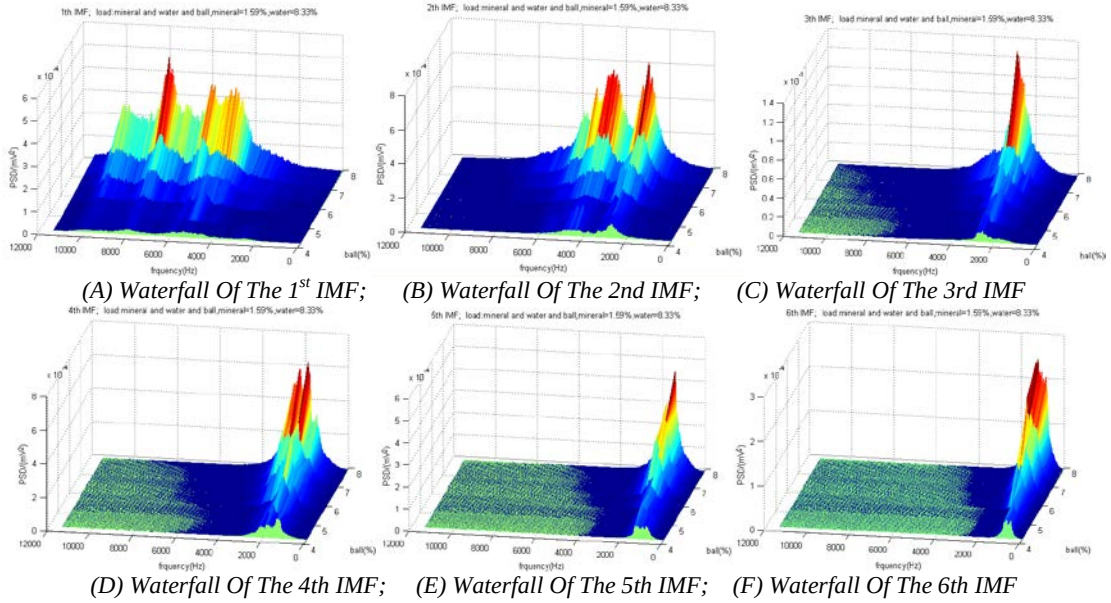

(A) Waterfall Of The 1st IMF; (B) Waterfall Of The 2nd IMF; (C) Waterfall Of The 3rd IMF

(D) Waterfall Of The 4th IMF; (E) Waterfall Of The 5th IMF; (F) Waterfall Of The 6th IMF

Figure 5: PSD Waterfalls Of The Former Six Imfs With Ball Load Increase

ISSN: 1992-8645 www.jatit.org E-ISSN: 1817-3195

Fig.5 shows with the increase of the ball loads, the amplitudes of the every IMF at different frequency bands increase evidently. The changes of the load are embodied in every IMFs. Thus, the ball load information is contained in every IMFs. The reason is described in [11], which are omitted here.

However, in practice, the ball load changes less in the running of the grinding process in short time period. Thus, the monitor of the mill load parameters is very important. The analysis among the different IMFs and mill load parameters are done in the next sub-section.

3.2 Feature Analysis Of Intrinsic Mode Functions

Because PLS algorithm captures the maximal covariance between the input and output data using less latent variables, it is used to analysis the relationship between mill load parameters and frequency spectrum of IMF. The percent variances captured by the 1st latent variable (LV) are shown in Table. 2. Frequency spectral correlate coefficients and relative change coefficients of the former seven IMFs are shown in Table .3.

Table 2: Percent variance captured by the 1st latent variable (LV) of PLS Algorithm

	Original	1st IMF	2nd IMF	3rd IMF	4th IMF	5th IMF	6th IMF	7th IMF
Frequency spectrum	92.35	80.15	78.82	71.15	51.86	69.95	70.08	60.81
Material to ball volume ratio	10.69	15.49	23.07	16.98	22.01	9.36	7.64	9.37
Frequency spectrum	92.50	81.18	82.05	76.89	61.66	78.06	72.79	61.75
Pulp density	45.14	50.66	56.46	37.67	16.77	27.87	32.72	47.87
Frequency spectrum	92.46	80.43	82.59	77.93	57.47	79.36	74.64	66.04
Charge volume ratio	41.12	46.72	41.98	28.87	21.51	25.63	29.18	31.96

Table 3: Relative change coefficients of the IMFs to the original signal

		Original	1st IMF	2nd IMF	3rd IMF	4th IMF	5th IMF	6th IMF	7th IMF
Material to ball volume ratio	Frequency spectral correlate coefficients	0.1157	0.1933	0.2926	0.2386	0.4244	0.1338	0.1090	0.1540
	$\gamma_{j_{IMF}}$	-----	1.67	2.52	2.06	3.66	1.15	0.94	1.33
Pulp density	Frequency spectral correlate coefficients	0.4880	0.6240	0.6881	0.4899	0.2720	0.3570	0.4495	0.7752
	$\gamma_{j_{IMF}}$	----	1.27	1.41	1.00	0.55	0.73	0.92	1.58
Charge volume ratio	Frequency spectral correlate coefficients	0.4446	0.5808	0.5082	0.3704	0.3742	0.3229	0.3909	0.4839
	$\gamma_{j_{IMF}}$	----	1.30	1.14	0.83	0.84	0.72	0.87	1.08

Table.3 shows that (1) Different mill load parameters relate to different IMFs, for example, material to ball volume ratio relates to 2nd, 3rd and 4th, pulp density relates to 1st , 2nd , 3rd and 7th IMF, charge volume ratio relates to 1st , 2nd , 6th and 7th IMF; (2) After decompose the original vibration signal, more interesting information can be found in IMFs, for example, most of the values of relative change coefficients are larger than 1; (3) The most important IMFs are 1st, 2nd and 7th, whose frequency ranges are mainly 4,000~6,000Hz, 2,000~4,000Hz and 100~2000Hz respectively. Compare with the former research results [11], it is shows that 1st, 2nd and 7th IMF are caused by the secondary impaction, main impaction, and nature mode of the shell mechanical structure (consisting of mill load and mill shell) itself. However, all these analysis are based on the laboratory-scales ball mill with limited samples. More experiments and simulation will be done to validate the conclusions further. It has the potential advantages to measure the mill load parameters continuously to achieve better mill operation.

Journal of Theoretical and Applied Information Technology
15th November 2012. Vol. 45 No.1

ISSN: 1992-8645 www.jatit.org E-ISSN: 1817-3195

3.3 Mill Load Parameters Monitoring Based On Ensemble PLS

There are thirteen training samples to build soft sensor model of mill load parameters. Thirteen independent samples are used to test the soft sensor models. If the input data of the soft sensor model come from the original vibration signal, single IMF and several IMFs, the soft sensor model are named as ORI-PLS, IMF-PLS, IMF-EPLS model, respectively. The number of latent variables was determined with the leave-one-out across validation method. The real and estimate value curves of mill load parameters are shown in Figure 6.

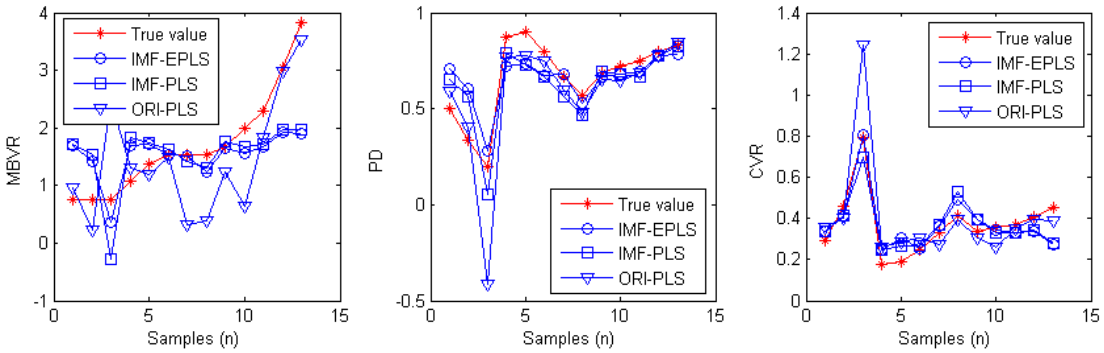

Figure 6: Prediction Results Of Different Approaches

The root mean square relative error (RMSSE) of different mill load parameters' models are shown in Table 4. In Table 4, the "ORI" presents the original vibration signal, whose length is four rotating period of ball mill; "RCS" represents relative change coefficients, which is defend in (13). With different "RCC" threshold, we select different IMFs to construct ensemble PLS models.

Table 4: Prediction accuracy and modeling parameters of different modeling approach

	Predictor Threshold: RCC	material to ball volume ratio (IMFs) latent variables	RMSSE	pulp density (IMFs) latent variables	RMSSE	charge volume ratio (IMFs) latent variables	RMSSE	RMSSE (Average)
ORI-PLS	ORI(100:12000)	5	0.7552	4	0.8548	2	0.2885	0.6328
IMF-PLS	IMF1(2000:12000)	2	0.6280	10	0.3338	2	0.2862	0.4160
	IMF2(1000:8500)	1	0.6503	3	0.3104	3	0.2309	0.3972
	IMF3(500:5500)	2	0.6344	11	0.6833	1	0.3420	0.5532
	IMF4(100:4000)	1	0.6250	1	0.4504	2	0.3483	0.4745
	IMF5(100:3000)	6	1.5251	9	0.4614	1	0.3608	0.7824
	IMF6(10:2000)	1	0.5227	1	0.4103	1	0.3106	0.6218
	IMF7(10:1000)	1	0.4584	2	0.3330	1	0.3593	0.3835
IMF-EPLS	RCC =0.5	(1,2,3,4,5,6,7)	0.5151	(1,2,3,4,5,6,7)	0.2907	(1,2,3,4,5,6,7)	0.3184	0.3747
	RCC =1.0	(1,2,3,4,5,7)	0.5454	(1,2,3,7)	0.3699	(1,2,7)	0.2946	0.4033
	RCC =1.1	**(1,2,3,4,5,7)**	**0.5454**	**(1,2,7)**	**0.3074**	**(1,2)**	**0.2527**	**0.3685**
	RCC =1.2	(1,2,3,4,7)	0.5351	(1,2,7)	0.3074	(1)	0.2862	0.3790
	RCC =1.3	(1,2,3,4,7)	0.5351	(2,7)	0.3056	1	0.2862	0.3756
	RCC =1.4	(1,2,3,4)	0.6189	(2,7)	0.3056	---	---	---
	RCC =1.5	(1,2,3,4)	0.6189	(7)	0.3330	---	---	---

The results show that ensemble PLS model with 'RCC =1.1" has the best average prediction accuracy. However, the best models for material to ball volume ratio, pulp density and charge volume ratio are IMF7-PLS, IMF-EPLS with "RCC =0.5" and IMF2-PLS. These mapping relationships between mill load parameters and IMFs are difference. It is very necessary to set different threshold. Compare with the relative change coefficients values in Table.3, it is shows IMFs with the biggest relative change coefficients has not the best prediction accuracy. The main reason

ISSN: 1992-8645 www.jatit.org E-ISSN: 1817-3195

is that the calculation of relative change coefficients is based on the first latent variables and the model is constructed with limited sample in abnormal condition. Moreover, only linear regression mode can be constructed using PLS algorithm. Thus, more suitable criterion and modeling algorithm should be researched to improve the prediction performance.

Modeling results show that IMF2 contain more information of pulp density and charge volume ratio. Fig.3, Fig.4 and Fig.5 show that the mainly frequency range of IMF2 is 2,000Hz to 6,000Hz, which mainly caused by the impaction of the mill load. For material to ball volume ratio, the prediction results are poorly. Studies show the shell acoustical signal has strong relationship with material to ball volume ratio. Thus, more signals should be fused in the future research. Further research will also address how to extract useful features from different IMFs to construct more powerful nonlinear soft sensor models.

4. CONCLUSIONS

The shell vibration signal of a laboratory scale ball mill is analyzed based on the EMD and PLS technologies. The ensemble PLS algorithm is used to construct mill load parameters and frequency spectrum of IMFs. The relationships between frequency spectrum of IMF and mill load parameters are described quantitatively by a new defined index. The following conclusions are drawn from the investigations: (1) Shell vibration signal can be decomposed into several sub-signals caused by different forces; (2) Cushion function of the water, mineral and pulp can be embodied in the time and frequency domain curves of different IMFs; (3) Some IMFs have more rich information on mill load parameters than original signals, and different mill load parameters are correlated with different IMFs; (4) Mill load parameters can be measured using EMD and EPLS based modeling approach.

However, the present research is based on laboratory ball mill. The physical interpretation of different IMFs cannot be explained clearly. More theoretically research and mill shell vibration simulation based on finite element analysis will be addressed. How to construct more effective soft sensor models based on EMD, feature extraction and selection method, and how to build effective nonlinear models are worth further study. More experiments will be done in the industry scale mill.

ACKNOWLEDGMENTS

The authors would like to acknowledge the financial support provided by the National Natural Science Foundation of China (61203102), National Science Foundation for Post-doctoral Scientists of China (No. 20100471464).

REFRENCES:

[1] G. Hu, H. Otaki, K. Watanuki., "Motion analysis of a tumbling ball mill based on non-linear optimization", Minerals Engineering, Vol. 13, No. 8-9, 2000, pp. 933-947.

[2] B. Behera, B. K. Mishra, C.V.R. Murty, "Experimental analysis of charge dynamics in tumbling mills by vibration signature technique", Minerals Engineering, Vol. 20, No. 1, 2007, pp. 84-91.

[3] J. Tang, T. Y. Chai, L. J. Zhao, W. Yu, H. Yue, "Soft sensor for parameters of mill load based on multi-spectral segments PLS sub-models and on-line adaptive weighted fusion algorithm", Neurocomputing, Vol. 78, No. 1, 2012, pp. 38-47.

[4] Y. Zeng, E. Forssberg, "Monitoring grinding parameters by vibration signal measurement-a primary application", Minerals Engineering, Vol. 7, No. 4, 1994, pp. 495-501.

[5] K. Gugel, G. Palcios, J. Ramirez, M. Parra, "Improving Ball Mill Control with Modern Tools based on Digital Signal Processing (DSP) Technology:", In: IEEE Cement Industry Technical Conference, Dallas, 4-9 May, 2003, pp. 311-318.

[6] S. J. Spencer, J. J. Campbell, K. R. Weller, Y. Liu, "Acoustic emissions monitoring of SAG mill performance", In: Proceedings of the Second International Conference on Intelligent Processing and Manufacturing of Materials, 1999, pp. 936-946.

[7] J. Tang, L. J. Zhao, J. W. Zhou, H. Yue, T. Y. Chai, "Experimental analysis of wet mill load based on vibration signals of laboratory-scale ball mill shell", Minerals Engineering, Vol. 23, 2010, pp. 720-730.

[8] J. Tang, L. J. Zhao, W. Yu, H. Yue, T. Y. Chai, "Soft sensor modeling of ball mill load via principal component analysis and support vector machines", Lecture Notes in Electrical Engineering, Vol. 67, 2010, pp. 803-810.

ISSN: 1992-8645 www.jatit.org E-ISSN: 1817-3195

[9] J. L. Liu, "On-line soft sensor for polyethylene process with multiple production grades", Control Engineering Practice, Vol. 15, 2007, pp. 769-778.

[10] L. J. Xu, X. M. Li, F. Dong, Y. Wang, L. A. Xu, "Optimum estimation of the mean flow velocity for the multi-electrode inductance flowmeter", Measurement Science and Technology, Vol. 12, 2001, pp. 1139-1146.

[11] N. E. Huang, S. R. Long and Z. Shen, "The mechanism for frequency downshift in nonlinear wave evolution", Advances in Applied Mechanics, Vol. 32, 1996, pp. 59-117.

[12] R. Q. Yan, R. X. Gao, "Rotary machine health diagnosis based on empirical mode decomposition", Journal of Vibration and Acoustics, Vol. 130, 2008, pp. 1-12.

[13] J. Tang, L. J. Zhao, H. Yue, W. Yu, T. Y. Chai, "Vibration analysis based on empirical mode decomposition and partial least squares", Procedia Engineering, Vol. 16, 2011, pp. 646-652.

[14] N. E. Huang, Z. Shen, S. R. Long, "A new view of nonlinear water waves: the Hilbert spectrum", Annu. Rev. Fluid Mech., Vol. 31, 1999, pp. 417-457.

[15] S. A. McInerny, Y. Dai, "Basic vibration signal processing for bearing fault detection", IEEE Transactions on education, Vol, 46, 2003, pp. 149-156.

[16] A. Höskuldsson, "PLS Regression Methods", Journal of Chemometrics, Vol. 2, 1988, pp. 211-228.

[17] L. K. Hansen, P. Salamon, "Neural network ensemble", IEEE Transaction Pattern Analysis and Machine Intelligence, Vol. 12, No. 10, 1990, pp. 993-1001.

[18] Z. Q. Su, W. D. Tong, L. M. Shi, X. G. Shao, W. S. Cai, "A partial least squares-based consensus regression method for the analysis of near-infrared complex spectral data of plant samples", Analytical Letters, Vol. 39, No. 2006, pp. 2073-2083.

[19] H. Dong, M. H. Moys, "Assessment of discrete element method for one ball bouncing in a grinding mill," International Journal of Mineral Processing, Vol. 65, No. 3-4, 2002, pp. 213-226.